Geomorphology 284 (2017) 142–155

Contents lists available at ScienceDirect

Geomorphology

journal homepage: www.elsevier.com/locate/geomorph

The timing and extent of Quaternary glaciation of Stok, northern Zanskar Range, Transhimalaya, of northern India

Elizabeth N. Orr [a,*], Lewis A. Owen [a], Madhav K. Murari [a], Sourav Saha [a], Marc W. Caffee [b,c]

[a] Department of Geology, University of Cincinnati, Cincinnati, OH 45221, USA
[b] Department of Physics and Astronomy/PRIME Laboratory, Purdue University, West Lafayette, IN 47906, USA
[c] Department of Earth, Atmospheric and Planetary Sciences, Purdue University, West Lafayette, IN 47906, USA

ARTICLE INFO

Article history:
Received 4 March 2016
Received in revised form 18 May 2016
Accepted 30 May 2016
Available online 31 May 2016

Keywords:
Zanskar Range
Cosmogenic nuclides
Glacier extent
ELA
Bedrock controls

ABSTRACT

The glacial history of three tributary valleys (Namlung, Gopal Kangri and Stok Kangri) of the Stok valley, south of the Indus valley in the northern sector of the Zanskar Range, northern India is characterized using geomorphic mapping and cosmogenic ^{10}Be surface exposure dating. The new glacial chronostratigraphy for the Stok valley is the first for the northern Zanskar Range and provides insights into the spatial variability of glaciation in the Himalayan-Tibetan orogen. This framework facilitates the understanding of the nature and the timing of landscape evolution and paleoenvironmental change in the Himalayan-Tibetan orogen. At least four glacial stages are evident within each of the tributary valleys of Gopal Kangri (M_{G1}–M_{G4}, youngest to oldest) and Stok Kangri (M_{S1}–M_{S4}) that feed into the Stok valley. With the exception of the M_{G4} glacial advance (~124 ka) in Gopal Kangri, the Stok valley has preserved evidence of glaciations from ~50 ka to the present. Equilibrium-line altitudes and glacier reconstructions for the Stok valley and its tributaries demonstrate that glaciations have become progressively less extensive through time. Former glacier extents of the Stok region are comparable in length with glacial advances during the last glacial cycle in eastern Zanskar and in the southern Ladakh Range to the south and north of the Indus valley, respectively. Landscape evolution in the study area has occurred across numerous glacial-interglacial cycles by a combination of glacial and fluvial processes and is similar to that of the Ladakh Range.

1. Introduction

The Himalayan-Tibetan orogen is the most glaciated region outside of the polar realms (Owen, 2009; Owen and Dortch, 2014). The orogen exhibits a remarkable amount of glacial evidence, including impressive landforms and successions of sediment, which provide insight into the dynamics of past glaciation (Owen et al., 2008). Determining the extent and timing of present and past glaciation is an essential component for the broader understanding of landscape evolution and paleoenvironmental change in the Himalayan-Tibetan orogen.

During the past few decades glacial chronostratigraphies have been constructed throughout the orogen, with the particular aim of examining the synchroneity of glaciation and investigating the driving forces behind glaciation (Owen and Dortch, 2014). Much of this research has been motivated by a wish to better understand the interaction of two major climatic systems: the south Asian summer monsoon and the mid-latitude westerlies (Benn and Owen, 1998). Variation in the influence of these systems throughout the Quaternary, coupled with climatic gradients and orographic effects have created strong precipitation gradients throughout the orogen. Changes to these gradients over time are considered to have had a major influence upon the nature and timing of glaciation of the Himalaya (Owen and England, 1998; Finkel et al., 2003; Bookhagen et al., 2005a; Owen et al., 2008). This glaciation has influenced the style and rate of landscape evolution of this orogen, involving processes of sediment transfer and erosion (Owen, 2010). More specifically, the glaciations exert a strong control upon the development of topography (Brozovic et al., 1997), influence tectonics (Zeitler et al., 2001; Willett, 2010) and climate (Molnar and England, 1990), condition mountain systems, focus erosion (Norton et al., 2010), and may limit fluvial incision (Korup and Montgomery, 2008).

The development of numerical dating methods, specifically terrestrial cosmogenic nuclide (TCN) surface exposure dating and optically stimulated luminescence (OSL) has advanced many of these studies (Owen et al., 2010). Owen and Dortch (2014) summarized the challenges and advances these studies have made but highlight that the Quaternary glacial history of the orogen still remains poorly defined, despite the growth in the number of glacial chronostratigraphies available.

The semi-arid western sector of the Himalayan-Tibetan orogen has become one of the most intensely studied regions of the mountain belt. Dortch et al. (2013) developed the first regional chronological

* Corresponding author.
E-mail address: orreh@mail.uc.edu (E.N. Orr).

http://dx.doi.org/10.1016/j.geomorph.2016.05.031
0169-555X/

framework for this area of the orogen, synthesizing local chronostratigraphies of the Transhimalaya, Pamir, and Tian Shan. They established a scheme whereby regional glacial advances/stages could be defined, which they called semi-arid western Himalayan-Tibetan stages (SWHTS), allocating them numbers from 1 back in time to 9. This research showed that the timing and nature of glaciation in this region are very complex (Dortch et al., 2013; Owen and Dortch, 2014). In particular, the maximum extent of glaciation and its timing is different over short distances within the orogen (10^{1-2} km; Owen and Dortch, 2014). This emphasizes the necessity for more detailed glacial chronostratigraphies to be developed in critical regions of the orogen such as the Zanskar Range, Transhimalaya. This is the focus of our paper where determining the glacial history of the Zanskar Range will aid in our understanding of factors that control glaciation within the Himalaya.

We examined the glacial record of Stok in the northern sector of the Zanskar Range of northern India (Fig. 1). The Stok study area is comprised of several tributary valleys (Gopal Kangri, Stok Kangri, and Namlung) that feed into the Stok valley, which in turn drains into the Indus River in Ladakh. Stok is located in close proximity to the Ladakh Range, which bounds the northern side of the Indus valley, a range with one of the best-developed and most extensive glacial chronostratigraphies for the Himalayan-Tibetan orogen (Owen et al., 2006; Dortch et al., 2013). This area allows us to examine the synchroneity in time and the differences in the style of glaciation between the ranges of Ladakh and Zanskar on the northern and southern sides of the Indus valley, respectively. This has particular implications for future research of how glaciation may effect landscape development across a small area of an active mountain belt.

Burbank and Fort (1985) provided the first study of the glacial geology and geomorphology of the valleys of the Ladakh and Zanskar Ranges. They identified four sets of moraines in the southern catchments of the Ladakh Range and the northern catchments of the Zanskar Range and argued that these moraines represented glacial advances since the global last glacial maximum (gLGM = global maximum ice volumes during the last glacial: 19–23 ka at chronozone level 1 or 18–24 ka at chronozone level 2 of Mix et al., 2001). Glacial stage names were assigned to each set of moraines and correlations between the mountain ranges were made based on morphostratigraphy.

Burbank and Fort (1985) did not have the benefit of numerical dating methods to define the timing of the moraine formation. They argued that more restricted glacial advances were observed in the northern Zanskar Range compared to those of the southern Ladakh Range because of the bedrock controls. They hypothesized that the unusual configuration of steeply dipping, resistant sandstones and conglomerates of northern Zanskar prevented significant down valley glacial advance; whereas the homogeneous granodiorite of the Ladakh Range has allowed glaciers to advance farther down valley. Their study is particularly significant because it was one of the first studies that highlighted the possibility of bedrock controls upon mountain glaciation (Mitchell and Montgomery, 2006; Dühnforth et al., 2010; Ward et al., 2012).

Subsequent research by Brown et al. (2002), Owen et al. (2006), and Dortch et al. (2013) developed comprehensive glacial chronostratigraphies of the Ladakh Range using cosmogenic ^{10}Be. These studies demonstrated that the moraines were far older than proposed by Burbank and Fort (1985). The gLGM moraines of Burbank and Fort (1985), for example, are now dated to 317 ± 57 ka (Dortch et al., 2013). The most conventional method for dating moraines has been radiocarbon dating. However, radiocarbon cannot be employed to build glacial chronostratigraphies within this region of the orogen owing to the scarcity of available organic material in sediments that is needed for this technique (Owen and Dortch, 2014). Optically stimulated dating

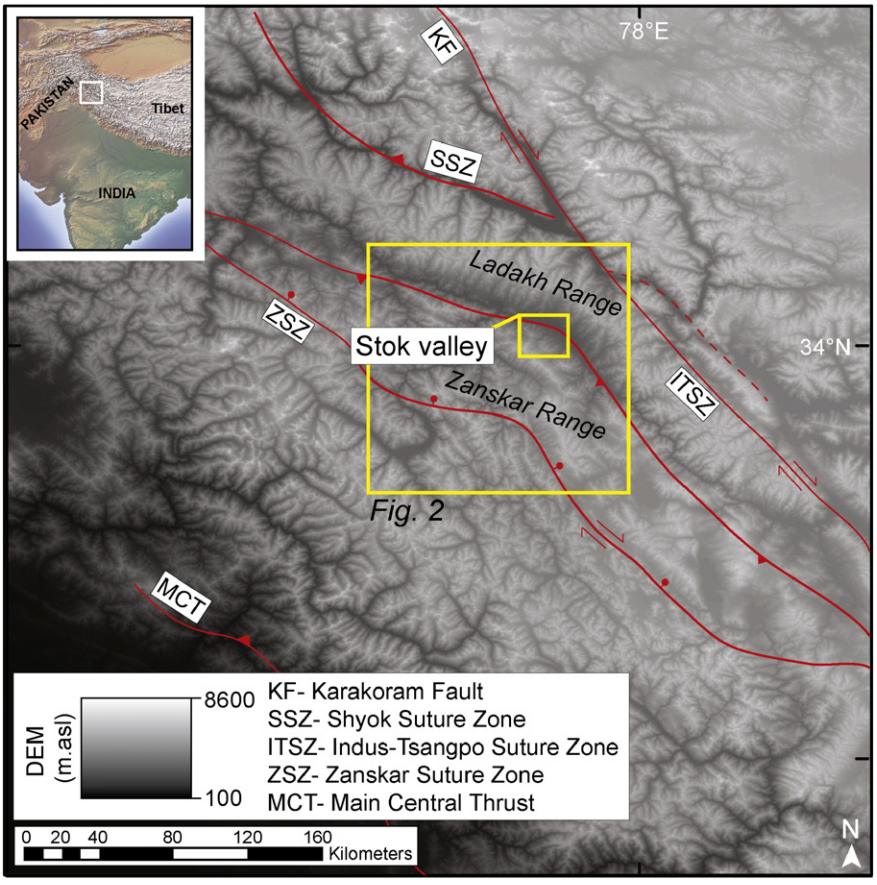

Fig. 1. Study area location over a Shuttle Radar Topography Mission (SRTM) DEM for the NW Himalaya. Major faults (red lines) from Hodges (2000). Inset image from www.geomapapp.org.

(OSL) has proved very difficult to apply in this region because of the low sensitivity of quartz, and the lack of appropriate sediments for dating (Owen and Dortch, 2014). Other dating techniques such as U-series, cannot be applied because of the lack of development of pedogenic carbonate in the sediments in this region.

The moraines of the northern catchments of the Zanskar Range, which border the Indus valley, have not been numerically dated. Given the large differences between the estimated ages of the Ladakh moraines of Burbank and Fort (1985) and the exposure ages for boulders on these moraines (Brown et al., 2002; Owen et al., 2006; Dortch et al., 2013), northern Zanskar's moraines are likely to be much older than the original estimates by Burbank and Fort (1985). Hedrick et al. (2011) for example, developed a glacial chronostratigraphy of the SE region of Zanskar, in which many of the moraine sets are older than the gLGM. Hedrick et al.'s (2011) study identified four glacial stages within each of the two valleys investigated; they tentatively identified asynchronous glaciation within this area of Zanskar. This and other recent work showing contrasting styles and timing of glaciation across regions of the Himalayan-Tibetan orogen, hint that correlations made across the Indus valley may be erroneous (Owen and Dortch, 2014).

Without robust glacial chronologies it is not possible to test whether bedrock may have had an influence upon glacier dynamics and in turn may affect the landscape evolution of Zanskar. Developing a detailed glacial chronostratigraphy on the northern side of the Zanskar Range will therefore shed light on the controls of glaciation throughout this region and help test whether bedrock configuration plays a principle role in the styles of glaciation. There has been considerable interest in developing geomorphic models for the Indus valley and the adjacent mountains (Hobley et al., 2010; Dortch et al., 2011; Blöthe et al., 2014; Dietsch et al., 2015), and our glacial chronology will provide a temporal framework for similar future studies. The three main tributary valleys (Namlung, Gopal Kangri, and Stok Kangri) that feed into Stok were mapped and cosmogenic nuclide methods were used to date well-preserved successions of moraines. Equilibrium-line altitudes (ELAs) were reconstructed to test the synchroneity and controls on glaciation between northern Zanskar and the southern Ladakh ranges.

2. Regional setting

The Zanskar Range, in which Stok is located, trends NE between the High Himalayan Divide and the Ladakh Range and rises from ~3500 m above sea level (asl) in the Indus valley to its highest peak, Stok Kangri at 6153 m asl (Fig. 1). The Zanskar Range formed during the continued collision of the continental Indian and Eurasian plates, resulting in the closure of the Neo-Tethys Ocean at ~55 Ma. These collision events formed the Zanskar Suture Zone (ZSZ) and Indus-Tsangpo Suture Zone (ITSZ) between the Zanskar and Ladakh ranges and were followed by a succession of structural events prior to ~36 Ma, resulting in the folding and thrusting of Zanskar metasedimentary rocks (Searle, 1986; Steck et al., 1998; Schlup et al., 2003; Fig. 2).

The Zanskar Range is a semi-arid, high altitude desert with desert steppe vegetation dominated by xerophytic shrubs and bushes (Fort,

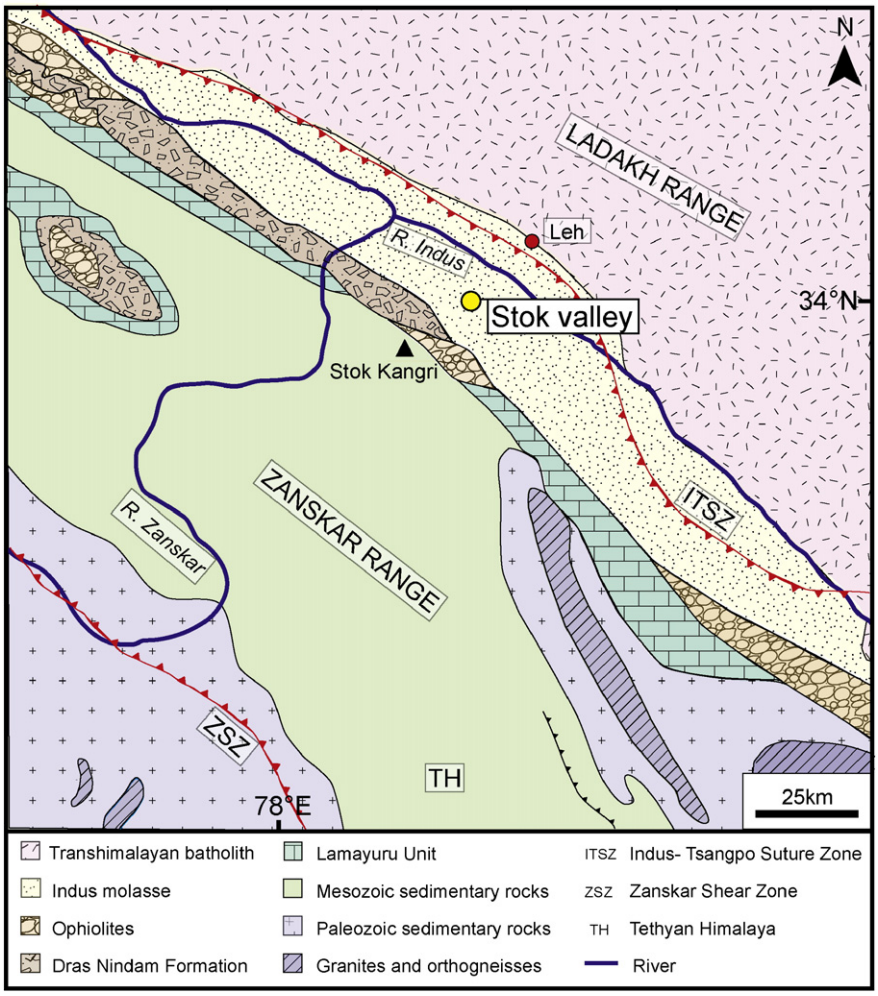

Fig. 2. Simplified geological map of northern Zanskar and southern Ladakh showing some of the major formations and geologic structures. Please see Brookfield and Andews-Speed (1984) for more detailed maps of the structures. Map has been modified from Steck et al. (1998) and Schlup et al. (2003). Fig. 1 shows the extent of this map.

1983; Taylor and Mitchell, 2000; Bookhagen et al., 2005b; Kamp et al., 2011). Zanskar's climate is primarily influenced by the south Asian monsoon and mid-latitude westerlies in the summer and winter, respectively (Benn and Owen, 1998; Owen et al., 2006). No specific climatic data is available for Zanskar; however Osmaston (1994) argued that data from the Leh Meteorological Station (34°09′N, 77°34′E, 3506 m asl) is representative of Zanskar's climate. The 30-year mean annual precipitation of Leh is 115 mm, ~40% of which falls between July and September of each year (Osmaston, 1994; Damm, 2006). The 12-year mean total annual rainfall data derived by the Tropical Rainfall Measuring Mission (TRMM) confirms this region to have an arid climate, measuring mean annual rainfall of <100 mm (Bookhagen and Burbank, 2010). In the city of Leh at an altitude of 3300 m asl, January and July temperatures range between −2.8–14 °C and 10.2–24.7 °C, respectively. With an environmental lapse rate of ~1 °C/170 m, we can conclude that for much of the Zanskar and Ladakh ranges the temperatures are significantly colder (Derbyshire et al., 1991).

Zanskar's climatic regime developed during the mid-Oligocene (~30 Ma) with the strong monsoonal influence taking affect at the beginning of the Miocene (~24 Ma; Clift et al., 2008). The intensity of the south Asian monsoon has fluctuated significantly throughout the Quaternary influencing the style and timing of glaciations and landscape change throughout the region (Sirocko et al., 1991; Benn and Owen, 1998; Bookhagen et al., 2005a).

Much of the Zanskar Range has remained unglaciated throughout the late Quaternary (Hedrick et al., 2011). Consequently, parts of the Ladakh region have preserved ancient preglacial landscapes where fluvial processes have primarily driven landscape evolution (Dietsch et al., 2015). For those valleys which have been glaciated, the glacial advances have remained confined to their respective catchments (Burbank and Fort, 1985; Mitchell et al., 1999). Many of these studied valleys have recorded between three and four glacial stages; many include glacial advances in the early part of the last glacial (many are the most extensive during the last glacial and are referenced to as the local last glacial maximum [lLGM]), gLGM, Lateglacial, Neoglacial, and Little Ice Age (Osmaston, 1994; Damm, 2006; Owen, 2009; Owen and Dortch, 2014). Lying in the rain shadow of the Himalaya, the contemporary glaciers of the Ladakh region are predominantly confined to north-facing headwalls and cirques and are of continental cold-based type (Benn and Owen, 2002; Dortch et al., 2011; Kamp et al., 2011; Owen, 2014).

Previous geomorphic studies of the Ladakh region have identified four major valley types: (i) heavily glaciated, wide valley with a cultivated valley floor; (ii) heavily glaciated, wide valley at higher altitudes with a noncultivated floor; (iii) narrow fluvial gorge; and (iv) a broad, gentle valley at high altitudes (Osmaston, 1994; Mitchell et al., 1999; Taylor and Mitchell, 2000; Hobley et al., 2010; Dietsch et al., 2015). Geological studies have described the high preservation of glacial, paraglacial, and periglacial landforms and deposits within these valleys. The landforms include moraines, terraces, debris fans, and mass movements (Taylor and Mitchell, 2000; Sant et al., 2011).

Stok is a collection of NE-trending tributary valleys at the most northerly extent of the Zanskar Range, ~7 km SW of the city of Leh (Fig. 1). Seven valleys sourced from the peaks of the Zanskar Range coalesce at ~4000 m asl and transition into the steep, narrow gorge of the Jingchan tributary. A large debris fan extends from the mouth of Stok onto the Indus River floodplain. Major river terraces are identified throughout the lower reaches, providing a record of paleofluvial activity. The valley slopes are either characterized by glacially polished bedrock or are mantled with extensive regolith with limited or no soil development.

3. Methodology

Four of the tributary valleys that feed into the Stok valley contain glaciers that extend <3 km from their respective headwalls. Three of Stok's valleys (Namlung, Gopal Kangri, and Stok Kangri) that exhibit the best-preserved succession of moraines also contain large till deposits and paraglacial landforms such as talus cones, debris fans, and mass wasting deposits and were studied in detail.

3.1. Field methods

Landforms in Stok were identified and mapped in the field, aided by topographic maps generated from a three arc-second (~90 m) Shuttle Radar Topography Mission (SRTM) digital elevation model. Present-day glacier extents were determined using field and Landsat ETM+ data (acquired in 2003) and Google Earth imagery.

Moraines in the three detailed study areas were divided on the basis of morphostratigraphy using the methodologies of Hughes et al. (2005) and Hughes (2010). High-relief moraines with well-defined crests and limited evidence of denudation were selected for dating. The sampled moraines were numbered in ascending order, from oldest to youngest. For example, the M_{G1} moraine in the Gopal Kangri valley (subscript G) is the youngest moraine (subscript 1), being the least weathered and at the terminus of the contemporary glacier. The M_{G4} moraine is the oldest of the four sets of moraines (subscript 4) and is located farthest downstream.

Boulders composed of quartz-rich lithologies – including granite, sandstone, and conglomerate – were selected for sampling. Where possible large, tabular, unweathered boulders that were well set into the crest of each moraine were chosen. Flat-topped boulders without debris cover were selected to avoid the need for any further shielding corrections other than topographic shielding. The location of each boulder was recorded using a hand-held Garmin Etrex 30 GPS unit.

A hammer and chisel was used to remove ~500 g (1–5 cm depth) of rock sample from the upper surface of each boulder. The characteristics of each boulder were recorded, including lithology, size, shape, weathering, emplacement, topographic shielding, and where appropriate, the dip and dip-direction of the sampled surface. Topographic shielding was measured using an inclinometer taking angle measurements from the boulder surface to the horizon at 10° azimuths.

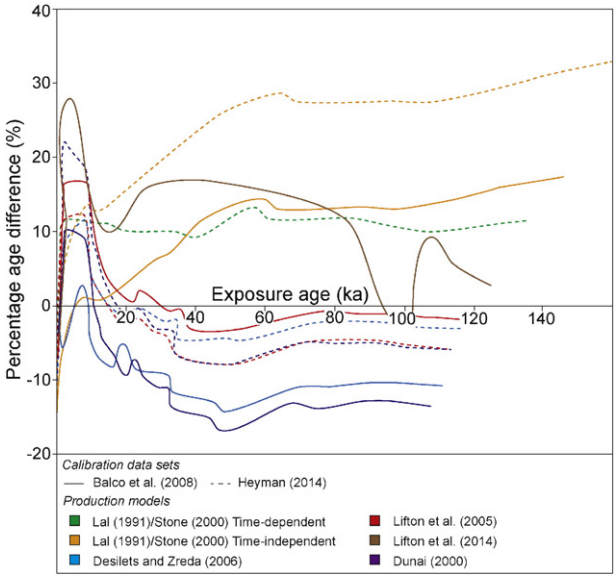

Fig. 3. Percentage age difference over the last 180 ka between the Lal (1991)/Stone (2000) time-dependent production rate model using Balco et al.'s (2008) global calibration data set and other age calculation schemes for the Stok's ^{10}Be data set. Other models include the Heyman (2014) calibration data set and Lal (1991)/Stone (2000) time independent, Lifton et al. (2005, 2014), Desilets and Zreda (2006), and Dunai (2000) production models.

3.2. Be-10 surface exposure dating

Samples were processed in the geochronology laboratories at the University of Cincinnati. Each sample was crushed and sieved to obtain the 250–500 μm fractions. Quartz isolation, dissolution, chromatography, isolation of Be, and preparation of BeO followed the methods of Kohl and Nishiizumi (1992) as described by Dortch et al. (2009). All samples were mounted onto steel cathodes and then the ratios of $^{10}Be/^{9}Be$ were measured at the Purdue Rare Isotope Measurement Laboratory (PRIME) at Purdue University.

Boulder ^{10}Be surface exposure ages were calculated using the CRONUS-Earth online calculator version 2.2 (Marrero et al., 2016). With the absence of a standardized age calculation scheme and regional calibration data set, the most appropriate production rate and scaling schemes for the Himalayan-Tibetan orogen remain unconfirmed. We utilized the Lal (1991)/Stone (2000) time-dependent production rate model using Balco et al.'s (2008) global calibration data set. This method has been successfully applied within this study region before (Dortch et al., 2013). With a theme of being thorough, we calculated ^{10}Be ages using the other available scaling schemes for comparison (Supplement item 1) and present the differences between these models and the Lal (1991)/Stone (2000) time-dependent in Fig. 3. The mean percentage difference between the models is <10%. The ages are calculated presuming no erosion, justifiable owing to the findings of Dietsch et al. (2015), who found that the glaciated catchments of the Ladakh Range undergo low erosion rates (<0.7 ± 0.1 m/Ma). On balance, we believe that these erosion rates are representative of the Zanskar Range. However, if we assume an erosion rate of 650–2480 m/Ma, then the age correction would be <2% for the Holocene, between 2 and 5% for the Lateglacial and gLGM, and >10% for ages over 40 ka (cf. Seong et al., 2007, 2009).

3.3. ELA reconstructions

The area-altitude (AA) method is considered to generate the best ELA estimates for the Himalayan-Tibetan orogen and is commonly supplemented by estimates using the area accumulation ratio (AAR) and toe-headwall accumulation ratios (THAR) (Benn et al., 2005; Osmaston, 2005). Our study follows the recommendations of Benn et al. (2005) and uses these methods to help reduce the uncertainties of the reconstructed ELAs. The mean value of the AA, AAR, and THAR methods are therefore used to estimate the ELAs for each of the glacial advances recorded within Stok. The ELAs were also reconstructed for southern Ladakh's glacial stages; the chronostratigraphy developed by Dortch et al. (2013). Each of the reconstructions is calculated using methodologies described by Osmaston (2005). The AARs of 0.4, 0.5, and 0.6 and THARs of 0.4 and 0.5 are used in this study because they have been shown to reflect accurate estimates within the Ladakh and the Karakoram ranges (Seong et al., 2008; Dortch et al., 2010). The

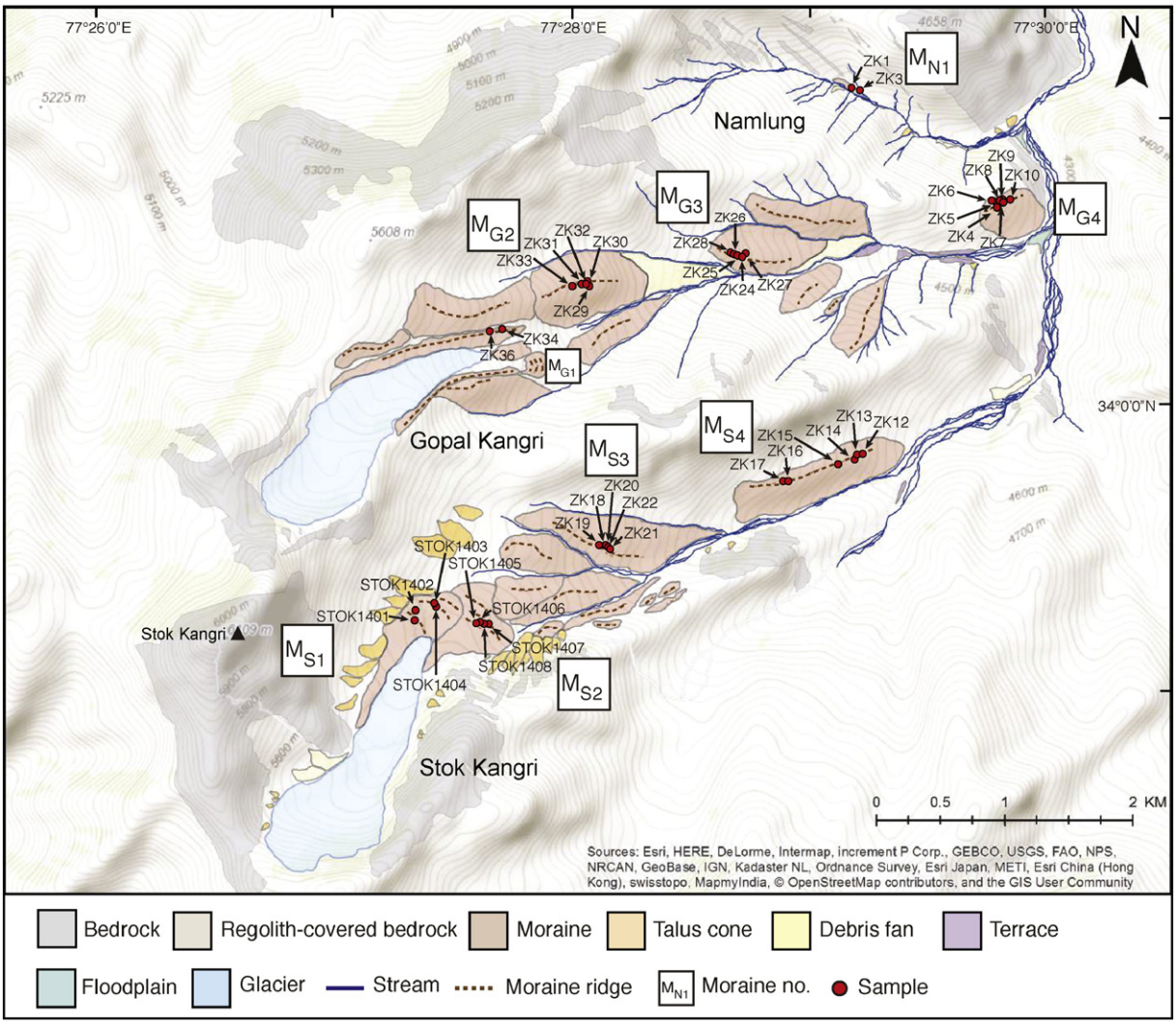

Fig. 4. Geomorphology of the Stok valley study areas, northern Zanskar Range, India.

ELA depressions (ΔELA) were calculated using the ELAs reconstructed using the AA method.

4. Details of study areas and landform descriptions

The three detailed study areas within the Stok valley are described in detail below (Fig. 4).

4.1. Namlung study area

The catchment of the Namlung tributary that drains from Namlung La (La = Pass) and trends NW is the most southerly study area in Stok. The Namlung study area is presently unglaciated and contains several debris fans, talus cone deposits, and a single moraine ridge (M_{N1}). Ridge M_{N1} is a small, sharply crested lateral moraine that is ~150 m long and is situated along the valley floor at ~4300 m asl. Large sub angular and striated boulders are sparsely distributed across the landform. The moraine ridge slopes are covered with a thick veneer of regolith.

4.2. Gopal Kangri study area

The Gopal Kangri valley is to the south of the Namlung valley. Downstream, the valley transitions from an ~5-km-long wide valley to one of an ~1.5-km-long gorge (Fig. 5). The catchment contains a small glacier that extends ~2 km. Gopal Kangri is characterized by a succession of moraines (M_{G1}, M_{G2}, M_{G3}, and M_{G4}) throughout the full catchment, including small recessional moraine ridges and larger lateral, latero-frontal, and terminal moraines.

M_{G4} is a large, latero-frontal moraine that is located ~3.6 km from the terminus of the contemporary glacier at the confluence between the Gopal and Jingchan rivers, ~1.2 km NW of M_{G3}. The moraine is composed of a pebbly diamicton with inset boulders sparsely distributed across this low relief landform. The boulders exhibit evidence of granular and cavernous weathering.

The M_{G3} moraine is 600 m long and is located 600 m NW from M_{G2} at ~4750 m asl. The moraine has a broad crest and is composed of a pebbly diamicton with a sandy-gravel matrix. Sub angular to rounded boulders with evidence of weathering are distributed across the full extent of the landform (Fig. 5).

M_{G2} is a latero-frontal moraine that is situated ~200 m NW of M_{G1}. This moraine is composed of a pebbly diamicton with a sandy gravel matrix, inset with sub angular to angular, moderately weathered boulders. A large debris fan feeds downstream in a NW direction from this subtle crested moraine at ~4800 m asl.

M_{G1} is a sharp-crested ~1.3-km-long lateral moraine that extends around the contemporary glacier. The landform and overlying boulders exhibit little evidence of weathering with some examples of rock spallation and polishing. Although the overlying boulders are distributed evenly across M_{G1}, many of these are not well set into the landform.

4.3. Stok Kangri study area

Stok Kangri is a SW-trending valley preserving a succession of moraines (M_{S1}, M_{S2}, M_{S3}, and M_{S4}) throughout the full extent of the valley. The valley's contemporary glacier extends from just below the Stok Kangri peak at ~6153 to ~5300 m asl. The landforms and deposits in

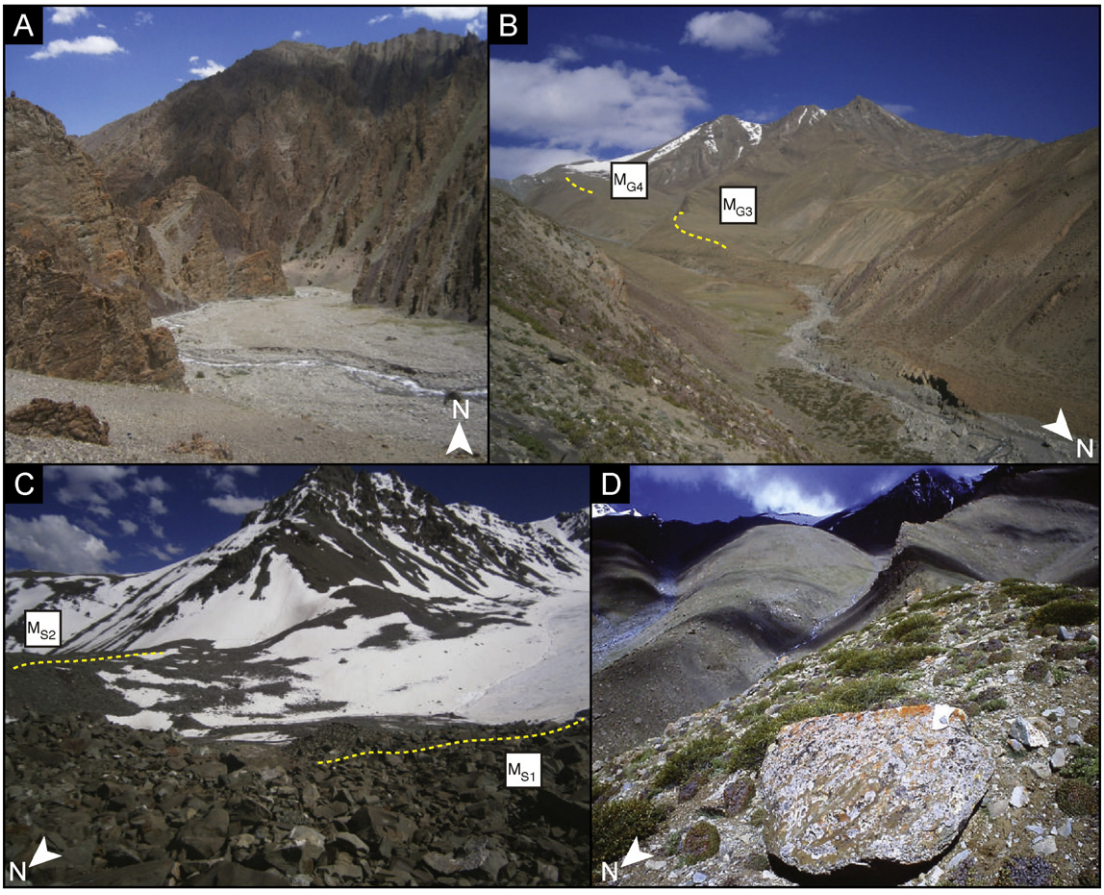

Fig. 5. Characteristic landforms in Stok. (A) View looking north, down the Stok valley toward the gorge at the lower reaches. (B) View SW up the Gopal Kangri catchment. M_{G2} and M_{G3} moraines are located of the western flanks of the catchment. Yellow dashed lines indicate the sampled moraine ridges of M_{G3} and M_{G4}. (C) View SE toward the contemporary Stok Kangri glacier. M_{S1} and M_{S2} moraines (moraine ridges indicated by yellow dashed lines) are located at the glacier's terminus. (D) Sampled boulder ZK28 from the M_{G3} moraine of the Gopal Kangri catchment.

Table 1
Sample details and 10Be ages (uncertainty is expressed as 1σ) for the moraines of Stok study area.

Sample name	Moraine	Moraine type	Location		Altitude	Boulder size			Lithology	Weathering	Sample thickness	Topographic shielding factor	^{10}Be	Minimum exposure age
			Latitude (°N)	Longitude (°E)	(m asl)	Length (m)	Width (m)	Height (m)			(cm)		(10^6 atoms/g)	(ka)
Namlung														
ZK1	M_{N1}	L	34.0184	77.4866	4407	0.5	0.4	0.2	Psammite	MB	2	1.00	1.61 ± 0.063	19.8 ± 1.9
ZK3	M_{N1}	L	34.0182	77.4869	4371	1.2	0.4	0.3	Conglomerate (SC), (P), (G, Q)	MB	3	1.00	0.59 ± 0.027	7.5 ± 0.8
Gopal Kangri														
ZK34	M_{G1}	LF	34.0043	77.4618	5280	2.5	0.8	1.3	Pebbly sandstone	MB	3	0.96	1.7 ± 0.2	1.5 ± 0.2
ZK36	M_{G1}	LF	34.0042	77.4610	5294	1.0	0.9	0.8	Conglomerate (SC), (P-C), (G)	SW	3	1.00	1.1 ± 0.2	1 ± 0.1
ZK29	M_{G2}	LF	34.0068	77.4679	5090	4.5	1.0	0.6	Conglomerate (SC), (P-C), (G, Q)	HW/HB	2	1.00	21.3 ± 2.6	21.1 ± 1.9
ZK30	M_{G2}	LF	34.007	77.4678	5095	1.3	0.6	1.0	Quartzite	DB	3	1.00	23.8 ± 2.8	22.1 ± 1.9
ZK31	M_{G2}	LF	34.0069	77.4674	5113	4.0	1.0	1.2	Conglomerate (SC), (C), (G)	SW/DB	2	1.00	39.1 ± 4.7	37.5 ± 3.3
ZK32	M_{G2}	LF	34.0043	77.4618	5280	0.8	0.6	1.1	Pebbly sandstone	MW/DB	3	1.00	13.5 ± 1.7	13.1 ± 1.3
ZK33	M_{G2}	LF	34.0068	77.4667	5128	1.0	1.0	0.7	Sandstone	MB	2	1.00	14.2 ± 1.7	12.5 ± 1.1
ZK24	M_{G3}	L	34.0085	77.4786	4755	1.5	0.3	1.2	Pebbly sandstone	SW/SB	2	0.98	32.2 ± 4.1	29.7 ± 2.9
ZK25	M_{G3}	L	34.0086	77.4783	4767	1.7	0.5	0.6	Pebbly sandstone	SW/MB	2	0.96	26.2 ± 3.2	23.8 ± 2.2
ZK26	M_{G3}	L	34.0086	77.4782	4769	1.2	0.4	0.7	Quartzite	MB	3	0.97	27.3 ± 3.4	26.9 ± 2.6
ZK27	M_{G3}	L	34.0087	77.4788	4755	1.3	1.0	0.9	Conglomerate (SC), (P-C), (G, Q)	SW/MB	3	1.00	32.0 ± 3.9	29.5 ± 2.6
ZK28	M_{G3}	L	34.0087	77.4779	4766	1.8	1.0	4.0	Pebbly sandstone	MW/MB	3	0.96	35.2 ± 4.2	32.6 ± 2.8
ZK4	M_{G4}	T	34.0113	77.4965	4434	1.3	0.6	0.5	Conglomerate	HW/DB	2	1.00	106.3 ± 13.0	99.9 ± 8.8
ZK5	M_{G4}	T	34.0117	77.4964	4438	2.0	2.0	0.3	Pebbly sandstone	MB	2	1.00	107.8 ± 14.1	109.7 ± 10.9
ZK6	M_{G4}	T	34.0118	77.4961	4439	2.2	1.6	0.5	Conglomerate (SC), (P-C), (G)	HB	3	1.00	132.5 ± 16.2	124.3 ± 11
ZK7	M_{G4}	T	34.0118	77.4968	4447	4.5	2.5	0.1	Conglomerate (SC), (P-C), (G)	MW/DB	2	1.00	114.7 ± 14.0	108 ± 9.5
ZK8	M_{G4}	T	34.0117	77.4967	4425	1.2	0.4	0.7	Conglomerate (SC), (P-C), (G, Q)	MW/MB	3	1.00	85.3 ± 11.2	86.4 ± 8.7
ZK9	M_{G4}	T	34.0117	77.4969	4426	3.3	2.0	1.0	Pebbly sandstone	MW/MB	2	1.00	106.6 ± 13.1	100.1 ± 9
ZK10	M_{G4}	T	34.0118	77.4974	4417	1.8	0.8	0.5	Pebbly sandstone	SB	2	1.00	84.0 ± 10.2	77.7 ± 6.8
Stok Kangri														
STOK1401	M_{S1}	LF	33.9873	77.4557	5329	1.0	0.8	0.6	Porphyritic granite	MW/MB	3	0.96	0.15 ± 0.051	1.7 ± 0.2
STOKl402	M_{S1}	LF	33.9879	77.4557	5330	2.1	1.7	0.6	Porphyritic granite	MB	3	1.26	0.12 ± 0.058	1.3 ± 0.1
STOKl403	M_{S1}	LF	33.9883	77.4570	5323	2.1	2.1	1.1	Porphyritic granite	MB	4	1.26	0.15 ± 0.065	1.6 ± 0.1
STOKl404	M_{S1}	LF	33.9882	77.4571	5328	2.2	1.0	0.8	Metagranite	SW/MB	2	1.24	0.21 ± 0.0086	0.2 ± 0.02
STOKl405	M_{S2}	T	33.9872	77.4601	5370	1.5	1.3	0.5	Metagranite	SW	2	1.26	0.076 ± 0.0031	0.8 ± 0.1
STOKl406	M_{S2}	T	33.987	77.4600	5314	2.6	2.1	0.8	Metagranite	SB	2.5	1.25	0.045 ± 0.0022	0.5 ± 0.04
STOK1407	M_{S2}	T	33.9871	77.4608	5340	1.1	0.9	0.5	Metagranite	SW/MB	3	1.26	0.012 ± 0.0021	0.1 ± 0.02
STOKl408	M_{S2}	T	33.9871	77.4606	5308	1.2	0.9	0.5	Metagranite	SB	3	1.01	0.093 ± 0.0072	1 ± 0.1
ZK18	M_{S3}	LF	33.9917	77.4689	5103	2.0	0.9	1.2	Conglomerate (SC), (P), (G, Q)	HW/DB	3	0.96	21.4 ± 2.6	19.6 ± 1.7
ZK19	M_{S3}	LF	33.9917	77.4686	5104	1.2	1.0	0.9	Pebbly sandstone	HW/DB	3	1.00	23.8 ± 2.8	22.04 ± 1.9
ZK20	M_{S3}	LF	33.9917	77.4690	5098	3.0	2.0	0.8	Psammite	HW/DB	4	1.00	18.0 ± 2.2	17.7 ± 1.6
ZK21	M_{S3}	LF	33.9915	77.4693	5097	3.5	1.5	1.2	Pebbly sandstone	SW/DB	2	0.98	12.5 ± 1.5	10.8 ± 1
ZK22	M_{S3}	LF	33.9917	77.4691	5090	2.5	0.5	0.8	Pebbly sandstone	DB	2	0.98	11.4 ± 1.4	10.02 ± 0.9
ZK12	M_{S4}	L	33.997	77.4870	4676	2.5	1.7	0.6	Pebbly sandstone	MW/DB	2	1.00	38.0 ± 5.1	35.9 ± 3.8
ZK13	M_{S4}	L	33.9969	77.4866	4688	3.0	1.7	0.7	Conglomerate (SC), (P), (G, Q)	MW/DB	3	1.00	52.5 ± 6.5	52.01 ± 4.7
ZK14	M_{S4}	L	33.9967	77.4865	4695	1.4	1.4	1.2	Psammite	DB	2	1.00	24.4 ± 3.2	23.8 ± 2.4
ZK15	M_{S4}	L	33.9964	77.4853	4733	4.5	2.5	2.8	Pebbly sandstone	DB	3	1.00	56.0 ± 6.8	56 ± 5
ZK16	M_{S4}	L	33.9954	77.4818	4827	1.5	0.5	0.5	Sandstone	SW/MB	3	1.00	2.4 ± 0.3	2.1 ± 0.2
ZK17	M_{S4}	L	33.9954	77.4815	4817	1.0	0.5	0.4	Quartzite	MW/MB	3	1.00	28.8 ± 8.6	26.1 ± 7.5

Moraine type: L- lateral, LF- latero-frontal, T- terminal.
Conglomerate description: SC- siliceous cement, P- pebble sized clasts, C- cobble sized clasts, G- granitic clasts, Q- quartzite clasts.
Boulder weathering characteristics: SW- slightly weathered (no pitting), MW- moderately weathered (some pitting, moderate exfoliation), HW- highly weathered (exfoliated sheets can be manually pulled off the rock), SB- slightly buried, MB- moderately buried, DB- deeply buried.
Production rate for the CRONUS calculator is $5.10 \pm 0.26 \times 10^{-7}$ ^{10}Be atoms/grams SiO_2/year and a ^{10}Be half-life of 1.36 Ma.
Minimum exposure age is calculated used Balco et al. (2008) calibration dataset and Lal (1991)/Stone (2000) time dependent calculation scheme.

this valley exhibit increased weathering with distance downstream: from sharply crested moraines covered in angular boulders to more subdued, denuded landforms with rounded boulders with evidence of granular and cavernous weathering.

M_{S4} is a large, subdued lateral moraine nestled into the hillslope of the Stok Kangri catchment. This gravelly diamicton has an abundance of sub rounded to rounded boulders and weathered debris on its surface. The moraine is 1.1 km long and extends down valley from ~4800 to ~4500 m asl some 600 m NW of M_{S3}.

M_{S3} is a broad-crested lateral moraine located ~1 km NW of M_{S2}. The moraine is composed of pebbly diamicton and is 1.6 km long with moderately weathered, sub angular to rounded boulders distributed evenly across its surface. The M_{S3} moraine extends down valley from ~5150 to ~4850 m asl.

The M_{S2} moraine is made up of multiple ridges that exhibit no evidence of weathering. The moraine is located at the terminus of the glacier and extends 470 m down valley to an elevation of ~5200 m asl.

M_{S1} is a multiridged ~1-km-long terminal moraine located within 200 m of the contemporary glacier. The landform is a large unsorted deposit of boulders, cobbles, and gravel. Frost-shattered debris is evident across the moraine, although no signs of weathering of the landform or overlying debris is clear.

5. Age of landforms

Moraines in Stok yield ^{10}Be ages between ~0.2 and 124 ka (Tables 1 and 2; Fig. 6). These ages are described in detail for each study area below.

A significant effort was made to ensure that the boulders selected for sampling were likely to produce ^{10}Be ages representative of the minimum age of moraine formation and hence glaciation. Factors such as weathering, exhumation, and shielding by snow and/or sediment, moraine degradation, and boulder toppling can affect the ^{10}Be concentrations within rock surfaces and sediments and result in the underestimation of the age of the landform or deposit. Although Putkonen and Swanson (2003) and Heyman et al. (2011) argued that prior exposure only affects ~2% of all dated boulders, if the sampled boulders have been exposed to cosmic rays prior to moraine formation, the exposure ages are likely to be an overestimate of the true age. This is a problem that has been discussed at length by Owen (2009) and Heyman et al. (2011), where the combination of these factors can produce a large spread of ages for a single landform or deposit. To improve the resolution of glacial chronostratigraphies within the Himalayan-Tibetan orogen and other mountain belts, we collected multiple samples from each moraine to define the timing of landform development and to identify erroneously old or young boulder ages (Heyman et al., 2011). The ^{10}Be ages of this study should be considered as minimum age estimates for the sampled moraines.

Table 2
Summary of the moraine ages for the detailed study areas.

	No. of samples	Maximum age(ka)	Age range (ka)	Mean age (ka)
Namlung				
M_{N1}	2	19.8 ± 1.9	7–20	13.7 ± 2.9
Gopal Kangri				
M_{G1}	2	1.5 ± 0.2	1–2	1.3 ± 0.2
M_{G2}	6	37.5 ± 3.3	12–37	21.2 ± 4.5
M_{G3}	5	32.6 ± 2.8	24–33	28.5 ± 1.5
M_{G4}	7	124.3 ± 11	78–124	100.8 ± 5.8
Stok Kangri				
M_{S1}	4	1.7 ± 0.2	0–2	1.2 ± 0.3
M_{S2}	4	1 ± 0.1	0–1	0.6 ± 0.2
M_{S3}	5	22 ± 1.9	10–22	16 ± 2.4
M_{S4}	6	56 ± 5	2–56	38.7 ± 6.6

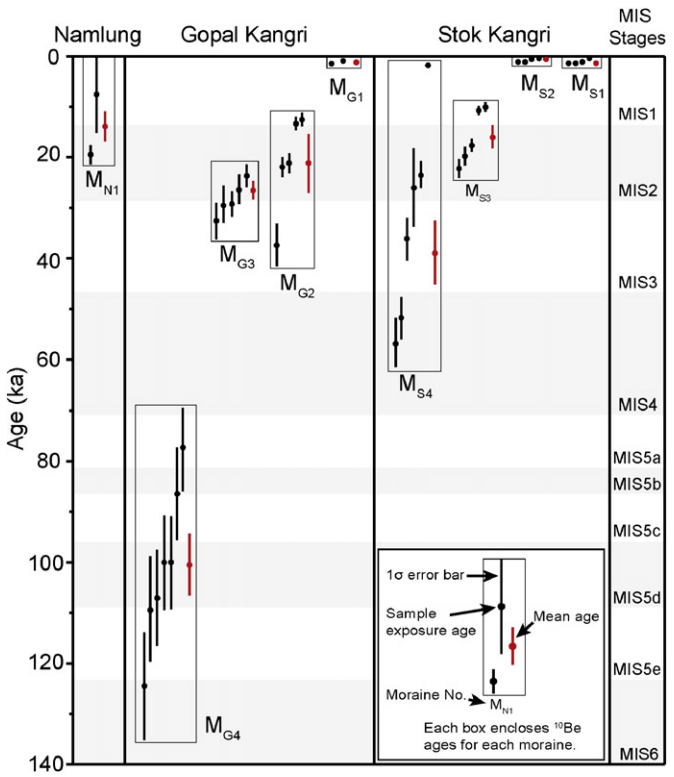

Fig. 6. Beryllium-10 ages for moraines in the Stok study areas (uncertainty is expressed as 1σ). Individual ^{10}Be ages for each moraine are plotted in descending order. Marine isotope stages derived from globally distributed benthic δ^{18}O records after Lisiecki and Raymo (2005).

5.1. Namlung study area

The single moraine, M_{N1}, in the Namlung study area yielded ^{10}Be ages of 19.8 ± 1.9 and 7.5 ± 0.8 ka. Additional sampling is required to constrain the timing of the moraine formation.

5.2. Gopal Kangri study area

The moraines sampled within this study area have distinct crests and are physically detached from one another. The ^{10}Be ages support the morphostratigraphy scheme we established, such that the morphostratigraphically older moraines have progressively older ^{10}Be ages.

The M_{G4} moraine has ^{10}Be ages between 78 and 124 ka (Fig. 6). This moraine has two major clusters of ages, the first between 100 and 125 ka and the second between 77 and 99 ka. The spread of ages could potentially signify the gradual stabilization or reworking of the landform at the onset of the last glacial cycle. This glacial advance may have occurred during the penultimate glacial cycle during marine oxygen isotope stage (MIS) 6.

The timing of the M_{G3} moraine is moderately well defined with five ^{10}Be ages that range from 24 to 33 ka with a mean boulder exposure age of 28.5 ± 1.5 ka.

The M_{G2} moraine has ages between 12 and 37 ka, a range that would be smaller if the oldest ^{10}Be age of 37.5 ± 3.3 ka is not considered (Fig. 6). This moraine has two major clusters of ages, the first between 19 and 24 ka and the second between 12 and 14 ka. The older cluster may represent the initial formation of the moraine with the younger cluster being the result of the stabilization or reworking of the landform and/or a later glacial stage.

Little confidence can be associated with the timing of the M_{G1} glacial advance based on the ^{10}Be dating because only two ^{10}Be boulder ages

(1.5 ± 0.2, 1.0 ± 0.1 ka) were determined for this moraine. Tentatively, the exposure ages suggest a recent glacial advance between 1 and 1.5 ka, with a mean age of 1.3 ± 0.2 ka (Fig. 6).

5.3. Stok Kangri study area

The ^{10}Be ages for Stok Kangri support the morphostratigraphy, whereby the progressively older morphostratigraphic moraines have the progressively older ^{10}Be ages. The only exception is between the M_{S1} and M_{S2} moraines. Although located higher within the valley, the M_{S1} exposure ages predate those of M_{S2}. The M_{S1} and M_{S2} moraines have mean exposure ages of 1.2 ± 0.3 and 0.6 ± 0.2 ka, respectively (Fig. 6). A likely explanation is that after the M_{S1} glacial stage, the glacier began to recede and exposed the M_{S1} lateral moraine along the headwall of Stok Kangri. The following, less extensive glacial stage then deposited the M_{S2} terminal moraine at a lower elevation within the valley.

The M_{S4} moraine has ^{10}Be ages ranging from 2 to 60 ka, with two clusters at 20–38 and 48–60 ka. The ZK16 sample's exposure age of 2.1 ± 0.2 ka is likely an outlier (Fig. 6).

The M_{S3} moraine has a mean age of 16 ± 2.4 ka with two ^{10}Be age clusters of 16 to 24 and 9 to 12 ka (Fig. 6). These clusters may represent two major phases of moraine development and stabilization.

6. Past ice extents and ELAs

The ELAs of Stok Kangri's glacial advances have gradually risen from ~5200 to 5500 m asl during the late Quaternary (Table 3; Fig. 7). In the past 100 ka, the glaciers of Gopal Kangri and Stok Kangri have each retreated a minimum of ~3 km upstream to present day positions and are now <3 km long. Gopal Kangri and Stok Kangri have contemporary ELAs that are within the uncertainty of Ladakh's regional ELA mean of 5455 ± 130 m asl (Dortch et al., 2011).

The mean and standard error of the AA, AAR, and THAR methods produce an ELA of 5496 ± 15.8 m asl for the contemporary glacier of the Gopal Kangri valley. The mean ELA for the valley's maximum recorded glacial advance (M_{G4}, ~78–124 ka) is 5025 ± 31.7 m asl, resulting in a ΔELA of ~469 m. The reconstructed ELA for the Stok Kangri contemporary glacier is 5537 ± 11.4 m asl. The mean ELA for the valley's maximum recorded glacial advance (M_{S4}, ~2–56 ka) is 5265 ± 38.1 m asl, producing a ΔELA of ~242 m. During this time, the M_{G3} glacial stage (~24–33 ka) of Gopal Kangri exhibits a comparable ΔELA of ~273 m.

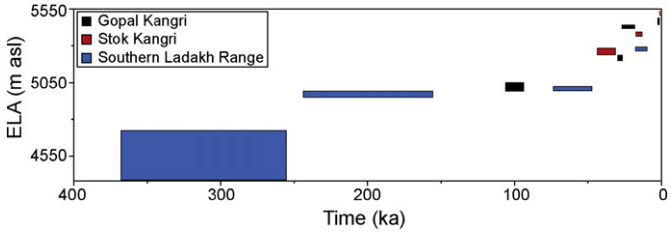

Fig. 7. Mean reconstructed ELAs of the late Quaternary glaciations of Gopal Kangri and Stok Kangri, northern Zanskar Range and the southern Ladakh Range (Owen et al., 2006).

The retreat of Gopal Kangri's glacial advances differ from Stok Kangri's gradual glacier retreat, with the recession of glacial ice punctured by a rapid ~300-m shift in ELA from 50 ka to present (Fig. 7). This is the only time where Gopal Kangri has exhibited a higher elevation ELA than Stok Kangri. Presently, Stok Kangri has a reconstructed ELA ~50m higher than Gopal Kangri.

7. Discussion

7.1. Stok valley chronology in the context of local and regional records

The detailed study areas within the Stok valley record evidence for glacial fluctuations over the past ~124 ka (Fig. 6). With the exception of the glacial advance in the Gopal Kangri study area that produced the M_{G4} moraine (~78–124 ka), the remainder of the glacial advances date to between ~0.2 and 50 ka. Stok contains no record of a glaciation during MIS 3 or 4, the local last glacial maximum (lLGM) that has been recognized elsewhere in the Himalayan-Tibetan orogen (Owen and Dortch, 2014). However, ^{10}Be ages between 48 and 60 ka for the M_{S4}

Table 3
Reconstructed ELAs for the northern Zanskar Range and the southern Ladakh Range.

	Glacier area	Headwall	Toe	Aspect	Area-altitude	Area-accumulation ratio			Toe-headwall altitude ratio		Mean ELA	ELA depression
	(km^2)	(m a.s.l)	(m a.s.l)		AA	AAR (0.4)	AAR (0.5)	AAR (0.6)	THAR (0.4)	THAR (0.5)	(m a.s.l)	(m)
Zanskar Range												
Namlung												
M_{N1}	3.9	5330	4430	E	4664	4699	4659	4619	4609.4	4659.5	4652 ± 12.2	–
Gopal Kangri												
M_{Gpres}	1.6	5900	5260	NE	5506	5549	5529	5490	5429.4	5474.5	5496 ± 15.8	–
M_{G1}	2.4	5900	5200	NE	5492	5549	5519	5489	5389.4	5434.5	5479 ± 21.6	~14
M_{G2}	4.5	5900	5130	NNE	5438	5489	5459	5419	5385.4	5449.5	5440 ± 13.2	~68
M_{G3}	11.7	5900	4720	NNE	5233	5310	5229	5159	5151.4	5259.5	5224 ± 22.5	~273
M_{G4}	20.6	5900	4350	NE	5037	5149	5049	4939	4917.4	5059.5	5025 ± 31.7	~469
Stok Kangri												
M_{Spres}	3.2	5850	5320	NNE	5536	5549	5519	5499	5535.4	5589.5	5537 ± 11.4	–
M_{S1}	4.3	5850	5300	NNE	5525	5509	5539	5469	5525.4	5584.5	5525 ± 14.1	~11
M_{S2}	4.2	5850	5290	NE	5501	5519	5489	5439	5515	5574	5506 ± 16.4	~35
M_{S3}	8.7	5850	4970	NE	5385	5429	5379	5329	5324	5415	5375 ± 16.1	~151
M_{S4}	11.6	5850	4575	NE	5294	5399	5320	5259	5095.4	5224.5	5265 ± 38.1	~242
Ladakh Range												
Khalling	6.5	5500	5130	WNW	5338	5369	5339	5309	5319	5355	5338 ± 8.3	–
Bazgo	16.8	5500	4735	WNW	5018	5079	5040	4989	4919	4964	5001 ± 21.2	–
Kar1	130.9	5500	4180	SSW	5082	5209	5130	4999	4775.4	4924.5	5020 ± 56	–
Kar2	104	5700	3930	SSW	5006	5159	5089	4999	4653.4	4834.5	4957 ± 68.6	–
Kar3	39.5	5730	4180	SW	4963	5119	4999	4869	4755.4	4899.5	4934 ± 46.1	–
Leh1	233.6	5600	3700	SSW	4801	5150	4900	4709	4503.4	4704.5	4795 ± 81.3	–
Leh2	99.2	5360	3570	S	4196	4339	4159	3979	4191.4	4364.5	4204 ± 51.9	–
Leh3	127.2	5700	3600	SSW	4878	5139	5049	4929	4437.4	4654.5	4848 ± 97	–
Leh4	203.7	5550	3600	SSW	4324	4450	4269	4099	4287.4	4499.5	4321 ± 53.1	–

moraine may represent an initial phase of landform development that may have coincided with this glacial advance.

The spread of ^{10}Be ages for each moraine prevents Stok's glacial advances from being compared statistically with each other to assess synchronicity. On Milankovitch timescales however, it is possible that the large degree of overlap of the ^{10}Be moraine ages could support the view that Stok's glacial advances were synchronous. It seems likely that the Gopal Kangri and Stok Kangri valleys were glaciated for the past ~50 ka.

Stok's glacial chronostratigraphy spans a smaller duration of time than other glacial chronologies local to the region (Table 2; Fig. 8). As an example, the Karzok valley of eastern Zanskar records a succession of glacial advances back to ~300 ka, a glacial chronostratigraphy that extends well into previous glacial cycles (Hedrick et al., 2011). Adjacent to Stok itself, the southern Ladakh Range has an established glacial chronostratigraphy that extends to >430 ka (Owen et al., 2006; Dortch et al., 2013). These observations are consistent with other records in close proximity to northern Zanskar, suggesting that rather

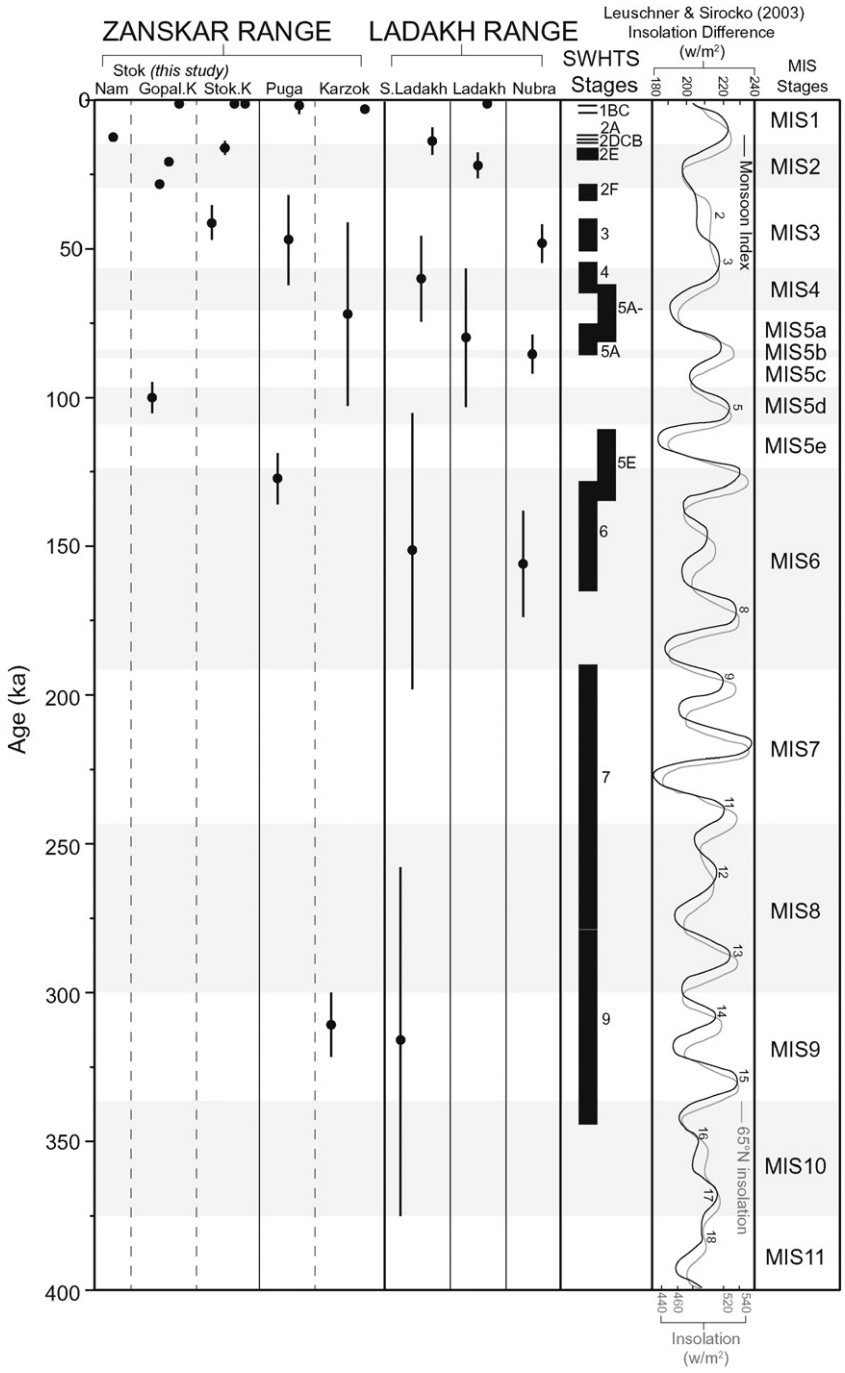

Fig. 8. Mean ^{10}Be moraine ages for Stok compared with local and regional studies. Individual ^{10}Be ages for each moraine are in descending order. ^{10}Be moraine ages from eastern Zanskar (Hedrick et al., 2011). ^{10}Be moraine ages from the southern Ladakh Range (Owen et al., 2006). ^{10}Be moraine ages from the Ladakh Range (Dortch et al., 2013). ^{10}Be moraine ages from northern Ladakh (Dortch et al., 2010). SWHTS stages derived from Dortch et al. (2013). Simulated monsoonal index and 65° N insolation of Leuschner and Sirocko (2003). Marine isotope stages derived from Lisiecki and Raymo's (2005) globally distributed benthic δ^{18}O records.

than a lack of glaciation prior to 124 ka, evidence of older glacial advances within Stok are missing because of subsequent erosion.

The M_{G4} glacial advance in Gopal Kangri likely occurred during the early part of the last glacial. Timing of glacial advances during this period has not been recognized within either local or regional chronologies thus far (Fig. 8). This glaciation may coincide with a period of greater monsoon and insolation intensity, conditions that have been correlated with periods of increased glaciation (Bookhagen et al., 2005a, 2005b).

The spread of ^{10}Be ages for each moraine in the Stok valley span several of the SWHTS stages from Dortch et al.'s (2013) regional framework, preventing any of Stok's advances from being correlated with a specific regional glacial stage (Fig. 8). For example, the timing of the M_{S3} glacial advance spans SWHTS 2E, 2D, 2C, and 2B. Possible explanations for this lack of coherence within the ^{10}Be ages for each moraine is that the landforms are the result of multiple phases of development or degradation or that they are composed of reworked material from previous glaciations or hillslope processes (Heyman et al., 2011).

Assigning glacial advances in Stok to specific climatostratigraphic events is ambiguous given our current dataset. Even on millennial timescales, the glaciations cannot be confidently correlated with periods of south Asian monsoon strengthening, increased insolation, or Northern Hemispheric climatic events (Owen, 2009). Unfortunately, this prevents this study from determining the potential climate mechanisms that force glaciation within this region.

7.2. Late Quaternary glaciation extents of northern Zanskar and southern Ladakh

Southern Ladakh preserves evidence of glaciations far older (>430 ka) than those recorded within Zanskar, which extends only to ~124 ka (Fig. 7). Between 10 and 100 ka when both ranges have recorded glaciations, glacial advances across Zanskar reached ~0.5–1 km farther down valley than Ladakh, relative to the present day glacier extents.

During the past 100 ka, the mean ELA in the southern Ladakh Range has retreated >404 m asl (4934 ± 46–5338 ± 8 m asl) relative to the present day; no contemporary glaciers reside in the valleys that contain the moraines that formulate southern Ladakh's glacial chronostratigraphy. During the winter, some ice may accumulate, although the true glacier extent cannot be defined. The mean ELA has retreated to a slightly greater extent of ~469 m asl (5025 ± 32–5496 ± 16 m asl) during the past 100 ka in the northern Zanskar Range. Northern Zanskar is able to support contemporary glaciers that extend <3 km down valley because the headwalls of Zanskar face north and are at higher elevations than the Ladakh Range's south-facing valleys.

Overall the former glacier extents, ELAs, and ΔELAs in northern Zanskar during the last glacial are similar to those in eastern Zanskar and the Ladakh Range (Owen et al., 2006; Dortch et al., 2010; Hedrick et al., 2011; Figs. 9 and 10). An important distinction is that in some of the regions that surround Zanskar, including Lahul and the Karakoram,

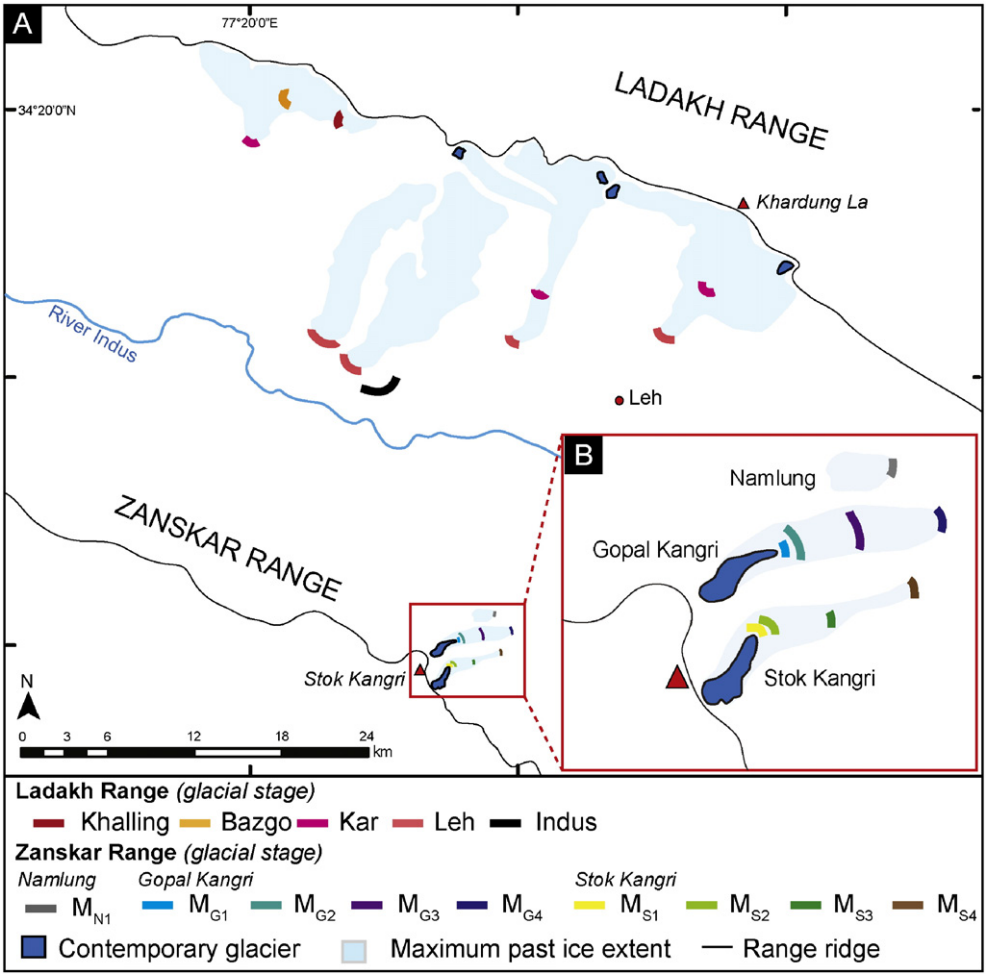

Fig. 9. (A) Map of the late Quaternary glaciation extents of the Zanskar and Ladakh ranges. (B) Enlarged image of the glaciation extents of the Stok valley, Zanskar.

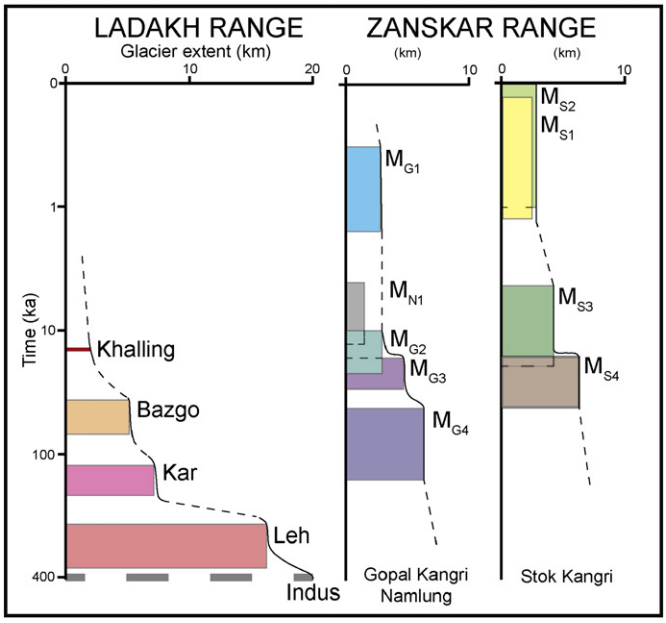

Fig. 10. Plots of the glacier extent of each glacial stage from the southern Ladakh Range and this study (Owen et al., 2006). Glacier extents are calculated from the contemporary ice limit. Black line delineates the estimated glacier extent for Zanskar and Ladakh from 0 to 400 ka. Dashed line highlights the uncertain glacier extents.

the glaciers have advanced >100 km during the last glacial. Owen et al. (2008) and Hedrick et al. (2011) have explained this transition in glaciation extent throughout the NW Himalaya as the consequence of strong climatic gradients and topographic controls.

7.3. The timing and extent of late Quaternary glaciation of Ladakh

Our study questions the view of Burbank and Fort (1985) that the Ladakh Range exhibits more extensive glacier limits than the Zanskar Range. Within the last ~100 ka it is estimated that the glacial advances of Stok and Zanskar were ~0.5–2 km more extensive, with ELAs ~50 m lower in elevation than the southern Ladakh Range (Fig. 10). Burbank and Fort (1985) argued that the Zanskar Range underwent less extensive glaciation because of the underlying bedrock restricting the advance of ice down catchment. This conclusion was made because the study assumed that the oldest moraines within both ranges represented an advance during the gLGM (Leh stage and M_{G4} moraines). The ^{10}Be ages of this study show that the gLGM moraines of Burbank and Fort (1985) are from different glacial periods, none of which coincided with the gLGM. The bedrock expressed in the northern Zanskar Range is unlikely to have been able to affect glacier dynamics sufficiently to control the extent of glaciation. Rather than acting as a barrier to glacier flow, the steep gorge morphology of Stok's lower reaches may have facilitated the convergence of the valley glaciers and steered glacial advances downstream (Peltier et al., 2000; Kessler et al., 2008).

The ^{10}Be dating of Stok's moraines demonstrate that rather than more restricted glaciation, there is no preserved evidence of glacial advances in the Stok valley prior to ~124 ka. Based upon the timing and maximum extents of glaciation in the Ladakh Range, it is likely that glaciers within Stok would have extended to the mouth of the Stok valley. There is the possibility that at a similar time to the Indus stage in Ladakh (>430 ka), Stok may have contained a glacier that also extended into the Indus valley itself. After this glacier retreated upstream, subsequent fluvial processes will have continued to calve the lower reaches of the Stok valley and develop the present gorge morphology, characteristic of the Ladakh region (Osmaston, 1994).

The lack of evidence of past glaciations in the lower reaches of the Stok valley is likely due to erosion. Significant erosion may have occurred during periods of deglaciation and paraglaciation where phases of continuous erosion and resedimentation of valley fills have reworked the moraines (Derbyshire and Owen, 1990; Benn et al., 2003). There is the possibility that the formation of the large debris fan at the mouth of the Stok valley may be as a consequence of paraglacial flooding (Ballantyne, 2002; Barnard et al., 2004, 2006). Alternatively, glacial advances from >124 ka may have been less extensive than those at the beginning of the last glacial cycle in the Stok valley, and so the evidence of these glacial stages has also been eroded away. We can conclude that the landscape evolution of Stok has occurred across numerous glacial-interglacial cycles by a combination of glacial and fluvial processes.

The Stok valley contains a record of multiple glacial advances throughout the last glacial. Our ages span a broad duration as a consequence of the large uncertainties associated with the dating method. This makes it challenging to match glacial advances with specific climatic events and mechanisms, such as periods of enhanced south Asian monsoon or Northern Hemispheric climatic cycles/events (Owen, 2009). Because these glaciers are small, continental, cold-based types we can speculate, that glacial advances in Stok are driven by small fluctuations in precipitation via the mid-latitude westerlies; a view proposed by Dortch et al. (2013) concerning the drivers of glaciations within the semi-arid sector of the Himalayan-Tibetan orogen. Furthermore, larger and less frequent glacial advances driven by the south Asian monsoon may be responsible for removing evidence of some of these smaller glacial events; limiting the glacial chronostratigraphy of Stok and other regions of the Himalaya to 3–4 glacial stages (Seong et al., 2009).

8. Conclusion

Terrestrial cosmogenic nuclide surface dating defines at least four glacial advances/stages within each of the valleys of Gopal Kangri and Stok Kangri. With the exception of the glacial advance that produced M_{G4} in the Gopal Kangri valley, the Stok valley have preserved evidence of glaciations between ~50 ka and the present day. The reconstructed glacial extents, ELAs, and ΔELAs for the Stok valley demonstrate that these glaciations have become progressively less extensive from the beginning of the glacial record to the contemporary glacier limits. The glacier extents of this study are consistent with glacial advances in eastern Zanskar and in the Ladakh Range (Owen et al., 2006; Dortch et al., 2010; Hedrick et al., 2011). Our study demonstrates that although the northern Zanskar and southern Ladakh ranges are within close proximity to one another, the duration and resolution of the glacial chronologies are different. Critically, this study shows that the style of glaciation between the Ladakh and Zanskar Ranges are not largely influenced by bedrock controls. Moreover, the development of this glacial chronology for the northern Zanskar Range may offer an opportunity in the future to address the present concerns of erroneous correlations made across the Indus valley, in terms of the style and timing of late Quaternary glaciation.

This study has emphasized the necessity of using numerical dating methods to define and interpret glacial chronologies within these ancient landscapes. Critically this study has developed the first comprehensive glacial chronostratigraphy of the northern Zanskar Range. Even so, it would be highly advantageous to investigate other valleys of the northern Zanskar Range, which have a longer glacial record than Stok has been able to preserve. This would facilitate a better comparison of the nature and timing of late Quaternary glaciation within and between the semi-arid mountain ranges of Ladakh and Zanskar, Transhimalaya.

Acknowledgements

ENO, LAO, MM, and SS would like to thank the Department of Geology at the University of Cincinnati for fieldwork support and for the

processing of samples for ^{10}Be dating in the geochronology laboratory facilities. MWC acknowledges support from NSF (EAR0844151). We should like to thank Dr. Richard Marston, Dr. Pradeep Srivastava and an anonymous reviewer for their detailed, constructive suggestions and comments on our manuscript.

Appendix A. Supplementary data

Supplementary data to this article can be found online at http://dx.doi.org/10.1016/j.geomorph.2016.05.031.

References

Balco, G., Stone, J., Lifton, N., Dunai, T., 2008. A complete and easily accessible means of calculating surface exposure ages or erosion rates from ^{10}Be and ^{26}Al measurements. Quat. Geochronol. 3, 174–195.
Ballantyne, C., 2002. Paraglacial geomorphology. Quat. Sci. Rev. 21, 1935–2017.
Barnard, P., Owen, L., Finkel, R., 2004. Style and timing of glacial and paraglacial sedimentation in a monsoon-influenced high Himalayan environment, the upper Bhagirathi Valley, Garhwal Himalaya. Sediment. Geol. 165, 199–221.
Barnard, P., Owen, L., Finkel, R., Asahi, K., 2006. Landscape response to deglaciation in a high relief, monsoon-influenced alpine environment, Langtang Himal, Nepal. Quat. Sci. Rev. 25, 2162–2176.
Benn, D., Owen, L., 1998. The role of the Indian summer monsoon and the mid-latitude westerlies in Himalayan glaciation: a review and speculative discussion. J. Geol. Soc. 155, 353–363.
Benn, D., Owen, L., 2002. Himalayan glacial sedimentary environments: a framework for reconstructing and dating the former extent of glaciers in high mountains. Quat. Int. 97–98, 3–25.
Benn, D., Kirkbride, M., Owen, L., Brazier, V., 2003. In: Evans, B. (Ed.), Glaciated Valley LandsystemsGlacial Landsystems. Routledge, pp. 372–406.
Benn, D., Owen, L., Osmaston, H., Seltzer, G., Porter, S., Mark, B., 2005. Reconstruction of equilibrium-line altitudes for tropical and sub-tropical glaciers. Quat. Int. 138–139, 8–21.
Blöthe, J.H., Munack, H., Korup, O., Fülling, A., Garzanti, E., Resentini, A., Kubik, P.W., 2014. Late Quaternary valley infill and dissection in the Indus River, western Tibetan Plateau margin. Quat. Sci. Rev. 94, 102–119.
Bookhagen, B., Burbank, D., 2010. Toward a complete Himalayan hydrological budget: spatiotemporal distribution of snowmelt and rainfall and their impact on river discharge. J. Geophys. Res. 115 (F3), 1–25.
Bookhagen, B., Thiede, R., Strecker, M., 2005a. Late Quaternary intensified monsoon phases control landscape evolution in the northwest Himalaya. Geology 33 (1), 149–152.
Bookhagen, B., Thiede, R., Strecker, M., 2005b. Abnormal monsoon years and their control on erosion and sediment flux in the high, arid northwest Himalaya. Earth Planet. Sci. Lett. 231, 131–146.
Brookfield, M., Andews-Speed, C., 1984. Sedimentology, petrography and tectonic significance of the shelf, flysh and molasses clastic deposits across the Indus-Suture Zone, Ladakh, NW India. Sediment. Geol. 40, 249–286.
Brown, E., Bendick, R., Bourles, D., Gaur, V., Molnar, P., Raisbeck, G., Yiou, F., 2002. Slip rates of the Karakorum fault, Ladakh, India, determined using cosmic ray exposure dating of debris flows and moraines. J. Geophys. Res. 107 (B9), 7–13, ESE 7-1–ESE.
Brozovic, N., Burbank, D.W., Meigs, A.J., 1997. Climatic limits on landscape development in the northwestern Himalaya. Science 276, 571–574.
Burbank, D., Fort, M., 1985. Bedrock control on glacial limits: examples from the Ladakh and Zanskar ranges, north-western Himalaya, India. J. Glaciol. 31 (109), 1430149.
Clift, P., Giosan, L., Blusztajn, J., Campbell, I., Allen, C., Pringle, M., Tebrez, A., Danish, M., Rabbani, M., Alizai, A., Carter, A., Luckge, A., 2008. Holocene erosion of the Lesser Himalaya triggered by intensified summer monsoon. Geology 36, 79–82.
Damm, B., 2006. Late Quaternary glacier advances in the upper catchment area if the Indus River (Ladakh and Western Tibet). Quat. Int. 154–155, 87–99.
Derbyshire, E., Owen, L., 1990. Quaternary alluvial fans in the Karakoram Mountains. In: Rachocki, A., Church, M. (Eds.), Alluvial Fans: a field Approach. Wiley, pp. 27–53.
Derbyshire, E., Shi, Y., Li, J., Zheng, B., Li, S., Wang, J., 1991. Quaternary glaciation of Tibet: the geological evidence. Quat. Sci. Rev. 10, 485–510.
Desilets, D., Zreda, M., 2006. Elevation dependence of cosmogenic ^{36}Cl production in Hawaiian lava flows. Earth Planet. Sci. Lett. 246, 277–287.
Dietsch, C., Dortch, J., Reynhout, S., Owen, L., Caffee, M., 2015. Very slow erosion and topographic evolution of the Southern Ladakh Range, India. Earth Surf. Process. Landf. 40 (3), 389–402.
Dortch, J.M., Owen, L.A., Haneberg, W.C., Caffee, M.W., Dietsch, C., Kamp, U., 2009. Nature and timing of mega-landslides in northern India. Quat. Sci. Rev. 28, 1037–1056.
Dortch, J., Owen, L., Caffee, M., 2010. Quaternary glaciation in the Nubra and Shyok valley confluence, northernmost Ladakh, India. Quat. Res. 74, 132–144.
Dortch, J., Owen, L., Schoenbohm, L., Caffee, M., 2011. Asymmetrical erosion and morphological development of the central Ladakh Range, northern India. Geomorphology 135, 167–180.
Dortch, J., Owen, L., Caffee, M., 2013. Timing and climatic drivers for glaciation across semi-arid western Himalayan-Tibetan orogen. Quat. Sci. Rev. 78, 188–208.
Dühnforth, M., Anderson, R., Ward, D., Stock, G., 2010. Bedrock fracture control of glacial erosion processes and rates. Geology 38 (5), 423–426.
Dunai, T.J., 2000. Scaling factors for production rates of in situ produced cosmogenic nuclides: a critical reevaluation. Earth Planet. Sci. Lett. 176, 157–169.
Fort, M., 1983. Geomorphological observations in the Ladakh Area (Himalayas): quaternary evolution and present dynamics. Contributsion to Himalayan Geology, Stratigraphy and Structure of Kashmir and Ladakh Himalaya. 2, pp. 633–652.
Finkel, R., Owen, L., Barnard, P., Caffee, M., 2003. Beryllium-10 dating of Mount Everest moraines indicates a strong monsoon influence and glacial synchroneity throughout the Himalaya. Geology 31 (6), 561–564.
Hedrick, K., Seong, Y., Owen, L., Caffee, M., Dietsch, C., 2011. Towards defining the transition in style and timing of Quaternary glaciation between the monsoon-influenced Greater Himalaya and the semi-arid Transhimalaya of Northern India. Quat. Int. 236, 21–33.
Heyman, J., 2014. Paleoglaciation of the Tibetan Plateau and surrounding mountains based on exposure ages and ELA depression estimates. Quat. Sci. Rev. 91, 30–41.
Heyman, J., Stroeven, A., Harbor, J., Caffee, M., 2011. Too young or too old: evaluating cosmogenic exposure dating based on an analysis of compiled boulder exposure ages. Earth Planet. Sci. Lett. 302, 71–80.
Hobley, D.E.J., Sinclair, H.D., Cowie, P.A., 2010. Processes, rates, and timescales of fluvial response in an ancient postglacial landscape of the northwest Indian Himalaya. Geol. Soc. Am. Bull. 122, 1569–1584.
Hodges, K., 2000. Tectonics of the Himalaya and southern Tibet from two perspectives. Geol. Soc. Am. Bull. 112, 324–350.
Hughes, P., 2010. Geomorphology and Quaternary stratigraphy: the roles of morpho-, litho- and allostratigraphy. Geomorphology 123, 189–199.
Hughes, P., Gibbard, P., Woodwad, J., 2005. Quaternary glacial records in mountain regions: a formal stratigraphical approach. Episodes 28, 85–92.
Kamp, U., Byrne, M., Bolch, T., 2011. Glacier fluctuations between 1975 and 2008 in the Greater Himalya Range of Zanskar, Southern Ladakh. J. Mt. Sci. 8, 374–389.
Kessler, M., Anderson, R., Briner, J., 2008. Fjord insertion into continental margins driven by topographic steering of ice. Nat. Geosci. 1, 365–369.
Kohl, C.P., Nishiizumi, K., 1992. Chemical isolation of quartz for measurement of in situ produced cosmogenic nuclides. Geochim. Cosmochim. Acta 56, 3583–3587.
Korup, O., Montgomery, D.R., 2008. Tibetan plateau river incision inhibited by glacial stabilization of the Tsangpo gorge. Nature 455, 786–789.
Lal, D., 1991. Cosmic ray labelling of erosion surfaces: in situ nuclide production rates and erosion models. Earth Planet. Sci. Lett. 104, 429–439.
Leuschner, D., Sirocko, F., 2003. Orbital insolation forcing of the Indian Monsoon- a motor for global climate changes? Palaeogeogr. Palaeoclimatol. Palaeoecol. 197, 83–95.
Lifton, N.A., Bieber, J.W., Clem, J.M., Duldig, M.L., Evenson, P., Humble, J.E., Pyle, R., 2005. Addressing solar modulation and long-term uncertainties in scaling secondary cosmic rays for in situ cosmogenic nuclide applications. Earth Planet. Sci. Lett. 239, 140–161.
Lifton, N., Sato, T., Dunai, T., 2014. Scaling in situ cosmogenic nuclide production rates using analytical approximations to atmospheric cosmic-ray fluxes. Earth Planet. Sci. Lett. 386, 149–160.
Lisiecki, L., Raymo, M., 2005. A Pliocene-Pleistocene stack of 57 globally distributed benthic δ18O records. Paleoceanography 20, 1.
Marrero, S., Philips, F., Borchers, B., Lifton, N., 2016. Cosmogenic nuclide systematics and the CRONUScale program. Quat. Geochronol. 31, 1–72.
Mitchell, W., Montgomery, 2006. Influence of a glacial buzzsaw on the height and morphology of the Cascade Range in central Washington State, USA. Quat. Res. 65 (1), 96–107.
Mitchell, W., Taylor, P., Osmaston, H., 1999. Quaternary geology in Zanskar, NW Indian Himalaya: evidence of restricted glaciation and preglacial topography. J. Asian Earth Sci. 307–318.
Mix, A.C., Bard, E., Schneider, R., 2001. Environmental processes of the ice age: land, ocean, glaciers (EPILOG). Quat. Sci. Rev. 20, 627–657.
Molnar, P., England, P., 1990. Late Cenozoic uplift of mountain ranges and global climatic change: chicken or egg? Nature 46, 29–34.
Norton, K.P., Abbühl, L.M., Schlunegger, F., 2010. Glacial conditioning as an erosional driving force in the Central Alps. Geology 38, 655–658.
Osmaston, H., 1994. In: Crook, J., Osmaston, H. (Eds.), The Geology, Geomorphology and Quaternary History of Zangskar. Himalayan Buddhist Villages 1, pp. 1–35.
Osmaston, H., 2005. Estimates of glacier equilibrium line altitudes by the Area × Altitude, the Area × Altitude Balance Ratio and the Area × Altitude Balance Index methods and their validation. Quat. Int. 138–139, 22–31.
Owen, L., 2009. Latest Pleistocene and Holocene glacier fluctuations in the Himalaya and Tibet. Quat. Sci. Rev. 28 (21–22), 2150–2164.
Owen, L., 2010. Landscape development of the Himalayan-Tibetan orogen: a review. Geol. Soc. Lond., Spec. Publ. 338, 389–407.
Owen, L.A., 2014. Himalayan landscapes of India. In: Kale, V.S. (Ed.), Landscapes and Landforms of India, World Geomorphological Landscapes. Springer Science-Business Media Dordrecht, pp. 41–52.
Owen, L., Dortch, J., 2014. Nature and timing of Quaternary glaciation in the Himalayan-Tibetan orogen. Quat. Sci. Rev. 88, 14–54.
Owen, L., Caffee, M., Bovard, K., Finkel, R., Sharma, M., 2006. Terrestrial cosmogenic nuclide surface exposure dating of the oldest glacial successions in the Himalayan orogen: Ladakh Range, northern India. GSA Bull. 118 (3–4), 383–392.
Owen, L.A., Caffee, M.W., Finkel, R.C., Seong, B.S., 2008. Quaternary glaciation of the Himalayan–Tibetan orogen. J. Quat. Sci. 23, 513–532.
Owen, L., England, J., 1998. Observations on rock glaciers in the Himalayas and Karakoram Mountains of northern Pakistan and India. Geomorphology 26, 199–213.
Owen, L., Yi, C., Finkel, R., Davis, N., 2010. Quaternary glaciation of Gurla Mandhata (Naimon'anyi). Quat. Sci. Rev. 29, 1817–1830.

Peltier, R., Goldsby, D., Kohlstedt, D., Tarasov, L., 2000. Ice age ice-sheet rheology: constraints from the Last Glacial Maximum form of the Laurentide ice sheet. Ann. Glaciol. 30, 1.

Putkonen, J., Swanson, T., 2003. Accuracy of cosmogenic ages for moraines. Quat. Res. 59, 255–261.

Sant, D., Wadhawan, S., Ganjoo, R., Basavaiah, N., Sukumaran, P., Bhattacharya, S., 2011. Morphostratigraphy and palaeoclimate appraisal of the Leh Valley, Ladakh Himalayas, India. J. Geol. Soc. India 77, 499–510.

Schlup, M., Carter, A., Cosca, M., Steck, A., 2003. Exhumation history of eastern Ladakh revealed by 40Ar/39Ar and fission-track ages: the Indus Rive- Tso Morari transect, NW Himalayas. J. Geol. Soc. 160, 385–399.

Searle, M., 1986. Structural evolution and sequence of thrusting in the High Himalayan, Tibetan-Tethys and Indus suture zones of Zanskar and Ladakh, Western Himalaya. J. Struct. Geol. 8 (8), 923–936.

Seong, Y.B., Owen, L.A., Bishop, M.P., Bush, A., Clendon, P., Copland, P., Finkel, R., Kamp, U., Shroder, J.F., 2007. Quaternary glacial history of the Central Karakoram. Quat. Sci. Rev. 26, 3384–3405.

Seong, Y.B., Owen, L.A., Bishop, M.P., Bush, A., Clendon, P., Copland, P., Finkel, R., Kamp, U., Shroder, J.F., 2008. Reply to comments by Matthias Kuhle on "Quaternary glacial history of the central Karakoram". Quat. Sci. Rev. 27, 1656–1658.

Seong, Y., Bishop, M., Bush, A., Clendon, P., Copland, P., Copland, L., Finkeel, R., Kamp, U., Owen, L., Shroder, J., 2009. Landforms and landscape evolution in the Skardu, Shigar and Braldu Valleys, Central Karakoram. Geomorphology 103, 251–267.

Sirocko, F., Sarnthein, M., Lange, H., Erlenkeuser, H., 1991. The atmospheric summer circulation and coastal upwelling in the Arabian Sea during the Holocene and last glaciation. Quat. Res. 36, 72–93.

Steck, A., Epard, J., Vannay, J., Hunziker, J., Girard, M., Morard, A., Robyr, M., 1998. Geological transect across the Tso Morari and Spiti areas- the nappe structures of the Tethys Himalayas. Eclogae Geol. Helv. 91, 103–121.

Stone, J.O., 2000. Air pressure and cosmogenic isotope production. J. Geophys. Res. 105, 23753–23759.

Taylor, P., Mitchell, W., 2000. The Quaternary glacial history of the Zanskar Range, northwest Indian Himalaya. Quat. Int. 65 (66), 81–99.

Ward, D., Anderson, R., Haeussler, P., 2012. Scaling the Teflon Peaks: rock type and the generation of extreme relief in the glaciated western Alaska Range. J. Geophys. Res. Earth Surf. 117, F1.

Willett, S.D., 2010. Erosion on a line. Tectonophysics 484, 168–180.

Zeitler, P., Meltzer, A., Koons, P., Craw, D., Hallet, B., Chamberlain, C., Kidd, W., Park, Seeber, L., Bishop, M., Shroder, 2001. Erosion, Himalayan Geodynamics, and the Geomorphology of Metamorphism. 4–9. GSA Today (Jan.).